International Journal of Science and Research (IJSR)
ISSN (Online): 2319-7064
Index Copernicus Value (2013): 6.14 | Impact Factor (2015): 6.391

Experimental Investigation the Effect of Weld Parameters on Mechanical and Metallurgical Properties of Dissimilar Joints AA6082–AA6061 in T6 Condition Produced by FSW

Vipul Chaudhari[1], Manish Rahevar[2]

[1, 2]Department of Mechanical Engineering, Parul University

Abstract: ***The effect of processing parameters on the mechanical and metallurgical properties of dissimilar joints of AA6082–AA6061 produced by friction stir welding was analysed in this study. Different FSW samples were produced by varying the welding speeds of the tool as 50 and 62 mm/min and by varying the alloy positioned on the advancing side of the tool. In all the experiments the rotating speed is fixed at 1600rpm. All the welds were produced perpendicularly to the rolling direction for both the alloys. Microhardness (HV) and tensile tests performed at room temperature were used to evaluate the mechanical properties of the joints. In order to analyse the microstructural evolution of the material, the weld's cross-sections were observed optically and SEM observations were made of the fracture surfaces. The corrosion tests of base alloy and welded joints were carried out in 3.5%NaCl solution at a room temperature. Corrosion current and potential were determined using potentiostatic polarization measurements. It was found that the corrosion rates of welded joints were higher than that of base alloy.***

Keywords: FSW; Aluminium alloys AA6082-AA6061; Mechanical and metallurgical characterization

1. Introduction

Modern aerospace concepts demand reductions in both the weight as well as cost of production of materials. Under such conditions, welding processes have proven most attractive, and programs have been set up to study their potential. Car manufacturers and shipyards are also evaluating new production methods. Increasing operating expenses are driving manufacturers to reduce weight in many manufacturing applications, particularly in aerospace sector. The goal is to reduce the costs associated with manufacturing techniques to result in considerable cost and weight savings by reducing riveted/fastened joints and part count. One way of achieving this goal is by utilising a novel welding technology known as Friction Stir Welding (FSW). Friction stir welding is a solid-state joining process developed and patented by the The Welding Institute (TWI) in 1991 by Thomas et al and it is emerged as a welding technique to be used in high strength alloys (2xxx, 6xxx, 7xxx and 8xxx series) for aerospace, automotive and marine applications that were difficult to join with conventional techniques[1,2]. This technique is attractive for joining high strength aluminium alloys since there is far lower heat input during the process compared with conventional welding methods such as Tungsten Inert Gas (TIG) or Metal Inert Gas (MIG). This solid state process leads to low distortion in long welds, excellent mechanical properties in the weld and heat-affected zone, no fumes or spatters, low shrinkage, as well as being energy efficient. Furthermore, other cost reductions are realized in that the process uses a non-consumable welding tool. The process was developed initially for aluminium alloys, but since then FSW was found suitable for joining a large number of materials.

In FSW a non-consumable rotating tool with a specially designed pin and shoulder is inserted into the abutting edges of sheets or plates to be joined and traversed along the line of joint. The tool serves two primary functions: (a) heating of work piece, and (b) movement of material to produce the joint. The heating is accomplished by friction between the tool and the work piece and plastic deformation of work piece. The localized heating softens the material around the pin and combination of tool rotation and translation leads to movement of material from the front of the pin to the back of the pin. As a result of this process a joint is produced in 'solid state'. During FSW process, the material undergoes intense plastic deformation at elevated temperature, resulting in generation of fine and equiaxed recrystallized grains. The fine microstructure in friction stir welds produces good mechanical properties. Fig. 1 shows a schematic diagram of the FSW process.

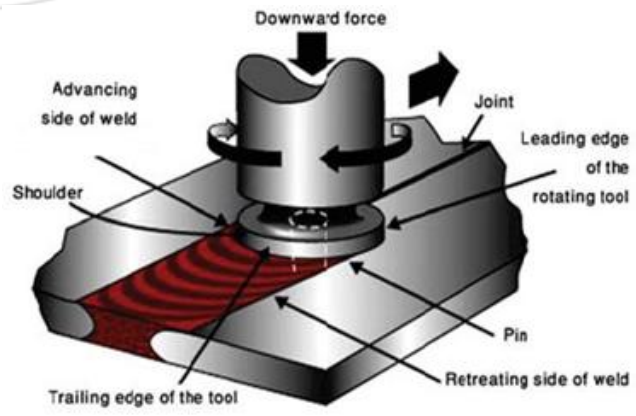

Figure 1: Schematic diagram of the FSW process

Many papers are present in the literature regarding this field. Further to joints of similar alloys, FSW is being studied for welding dissimilar alloys which can be of

particular interest in some industrial applications. Some works can be found in the literature [3–7], but data is still scarce on the characterisation of 6082-6061 joint type. Some authors have demonstrated that the microstructure of the weld nugget of strongly different aluminium alloys is mainly fixed at the retreating side of the material [3]. Murr et al. [8] showed the properties of dissimilar casting alloys by FSW. The micro- structural evolution of dissimilar welds as a function of processing parameters has been widely studied in [9], shows the behaviour of AA6061–AA2024 materials. Dickerson et al. [10] found that friction-stir-welded butt joints are generally defect free if welding process conditions (welding speed and sheet thickness) are properly tuned within a 'tolerance box' for a particular alloy. It is not possible to assume that FSW will be free of flaws, however, because manufacturers may want to run FSW outside the tolerance box in order to increase productivity.

The weld zones are more susceptible to corrosion than the parent metal [11-16]. Generally, it has been found that Friction stir (FS) welds of aluminium alloys such as 2219, 2195, 2024, 7075 and 6013 did not exhibit enhanced corrosion of the weld zones. FSW of aluminium alloys exhibit intergranular corrosion mainly located along the nugget's heat-affected zone (HAZ) and enhanced by the coarsening of the grain boundary precipitates. Coarse precipitates and wide precipitate-free zones promoted by the thermal excursion during the welding are correlated with the intergranular corrosion. The effect of FSW parameters on corrosion behaviour of friction stir welded joints was reported by many workers [14, 16]. The effect of processing parameters such as rotation speed and traverse speed on corrosion behaviour of friction stir processed high strength precipitation hardenable AA2219-T87 alloy was investigated by Surekha et al. [16]. However, researchers have nevertheless been strained to study competent study of the mechanical properties in terms of UTS, YS and % elongation, microhardness test, fractography analysis, metallurgical properties, and corrosion behaviour and the main causes of developing defects with changing FSW parameters for a dissimilar aluminium joint of AA6082 with AA6061. Selection of process parameters is an important issue in the FSW process, particularly in the case of joining dissimilar alloys. In the present paper, the effect of different welding speeds on the weld characteristics of advancing and retreating side of AA6082-T6 and AA6061-T6 fabricated by a hexagonal tool pin profile is investigated.

2. Experimental Procedure

The experiments were conducted on the aluminium alloy AA6082-T6 and AA6061-T6, its chemical composition and mechanical properties are respectively presented in Tables 1 and 2.

The rolled plates of 5mm thickness were cut into the required size (300mm×150 mm) by power hacksaw cutting and grinding. Square butt joint configuration was prepared to fabricate FSW joints. The initial joint configuration was obtained by securing the plates in position using mechanical clamps. The direction of welding was normal to the rolling direction. Single pass welding procedure was used to fabricate the joints. In present work hexagonal tool pin profile was used for the welds, made of cold work die steel. The tool dimensions are shown in Fig. 2. The machine used for the production of the joints was vertical machining centre. Different materials positioned on the advancing side of the tool allowed four different welding conditions described in Table 3.

Table 1: Chemical composition and mechanical properties AA6082-T6

Chemical Composition

Element	Si	Fe	Cu	Mn	Mg	Cr	Zn	Ti
Required	0.7-1.3	0.5	0.1	0.4-1.0	0.6-1.2	0.25	0.2	0.1
Contents	0.9	0.24	0.9	0.7	0.7	0.06	0.04	0.05

Mechanical Properties

Tensile Strength (MPa)		Yield Strength (MPa)		Elongation (%)		Hardness (HV)
Min	Max	Min	Max	Min	Max	
295	--	240	--	8	-	89
324	332	308	319	9	12	90

Table 2: Chemical composition and mechanical properties AA6061-T6

Chemical Composition

Element	Si	Fe	Cu	Mn	Mg	Cr	Zn	Ti
Required	0.4-0.8	0.7	0.15-	0.15	0.8-1.2	0.04-0.35	0.25	0.15
Contents	0.62	0.45	0.2	0.18	1.05	0.09	0.03	0.07

Mechanical Properties

Tensile Strength (MPa)		Yield Strength (MPa)		Elongation (%)		Hardness (HV)
Min	Max	Min	Max	Min	Max	
300	--	241	--	6	--	95
328.57	335.71	282	296	11	11.8	98

Table 3: Welding conditions employed to join the AA6082–AA6061 plates.

Materials of	Rotational	Welding	Tool	Downward
6082T6-6061T6	1600	50	4.6	14
6082T6-6061T6	1600	62	4.6	11
6061T6-6082T6	1600	50	4.6	11
6061T6-6082T6	1600	62	4.6	11

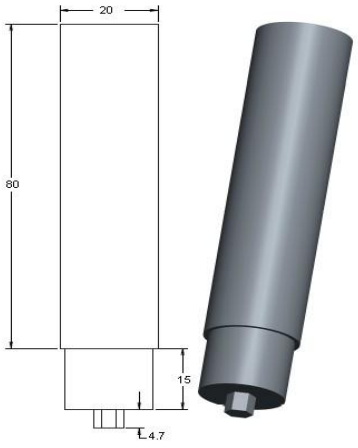

Figure 2: Geometry of the hexagonal tool pin profile used in the present study

All welded samples were visually inspected in order to verify the presence of possible macroscopic external defects, such as surface irregularities, excessive flash, and surface-open tunnels. By using Radiographic unit, X-Ray radiographic inspection was carried out on FSW samples. In radiographic test 6Ci & Ir192 used as radioactive source. The film used was Agfa D-4 and the radiographs indicated defect free weld as well as weld with defects like insufficient fusion and cavity. Mechanical properties of the test welds were assessed by means of tensile tests and the ultimate tensile stress (UTS) yield strength (YS) and % elongation were measured in the tensile test. Microindentation hardness test as per ASTM E-384:2006 has been used to measure the Vickers hardness of FSW joints. The Vickers microhardness indenter is made of diamond in the form of a square-base pyramid. The test load applied was 100gram and the dwell time was 15 seconds. The indentations were made at midsection of the thickness of the plates across the joint. The tensile fractured surfaces were analyzed by using scanning electron microscopy (SEM).

Metallographic specimens were cut mechanically from the welds, embedded in resin and mechanically ground and polished using abrasive disks and cloths with water suspension of diamond particles. The chemical etchant was the Keller's reagent. The microstructures were observed on optical microscope.

Potentiodynamic polarization tests were used to study the pitting corrosion behaviour of AA6082-AA6061 alloys. In the tests, cell current readings were taken during a short, slow sweep of the potential. The sweep was taken in the range of 0.5V to 1V. The potentiodynamic scan was performed at scan rate of 0.5mV/sec.

3. Result and Discussion

3.1 Mechanical Properties

The mechanical and metallurgical behaviour of dissimilar FSW AA6082–AA6061 was studied in this research. Transverse tensile properties of FSW joints such as yield strength, tensile strength, percentage of elongation and joint efficiency on transverse tensile specimens are presented in Tab. 4. The strength and ductility in the as-welded condition are lower than the parent metal in T6 condition.

Table 4: Mechanical properties of dissimilar FSW joints

Material of FSW Joint	*YS (N/mm^2)*	*UTS (N/mm^2)*	*% Elongation*	*% Joint Efficiency*
6082T6-6061T6	167	183	5.14	50.13-49.03
6082T6-6061T6	101	170	4	46.57-45.57
6061T6-6082T6	91	173	4.29	47.39-46.38
6061T6-6082T6	95	154	4.43	42.19-41.28
AA6082-T6	117	365	14	--
AA6061-T6	99.84	373.12	16.56	--

The joints were produced with different alloy positioned on the advancing side of the tool. The joints were realized with a rotation speed of 1600 rpm and by changing the advancing speed from 50 to 62 mm/min. From the Fig. 3 it can be inferred that the welding speed and alloy positions are having influence on tensile properties of the FSW joints.

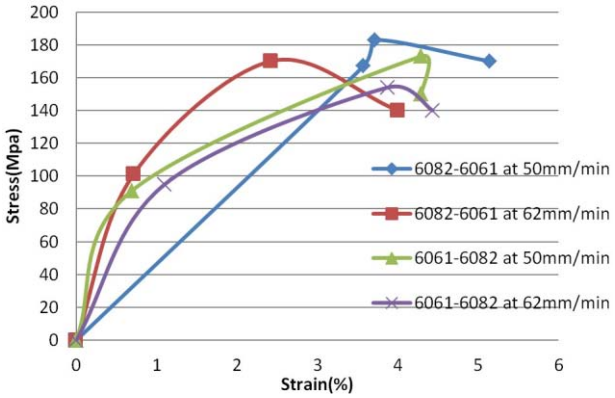

Figure 3: Stress-Strain curves for dissimilar alloys AA6082-AA6061.

The ductility is higher with decreasing the weld speed in the case of AA6082 on the advancing side, while it decreases in the case of AA6061 on the advancing side (Fig. 4). Such dependence of the strength on the material position was previously observed. The best conditions of strength and ductility are reached in the joints welded with AA6082 on the advancing side and weld speed of 50 mm/min. In joint efficiency table, the first efficiency represents the weld joint efficiency with AA6082 as a base metal and second efficiency represent with AA6061 as a base metal. The joint efficiency is higher with decreasing the weld speed in the case of AA6082 on the advancing side, while it is lower in the case of AA6061 on the advancing side. Fig. 5 shows the effect of welding speed on microhardness of dissimilar welds. The highest value of microhardness is reached in AA6061-6082 at welding speed of 50mm/min. The lowest value of microhardness is reached when the AA6061 alloy is on the advancing side of the tool at welding speed of 62 mm/min. When AA6082 alloy is employed on the advancing side of the tool, the microhardness appears more uniform, indicating a better mixing of the material as shown in Fig. 5. Furthermore, the maximum hardness values in the nugget zone correspond to the welds with AA6082 on the advancing side.

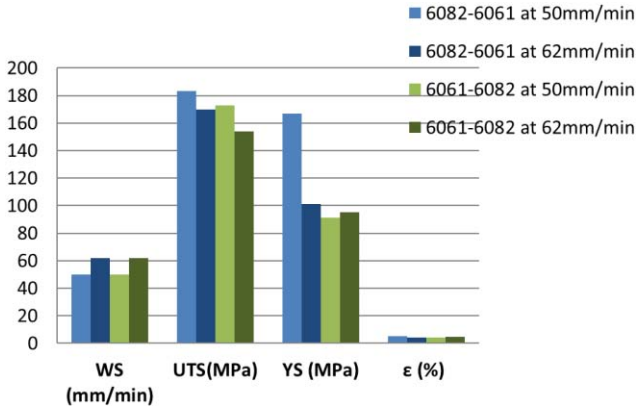

Figure 4: Effect of welding speed on mechanical properties for dissimilar alloys 6082-6061

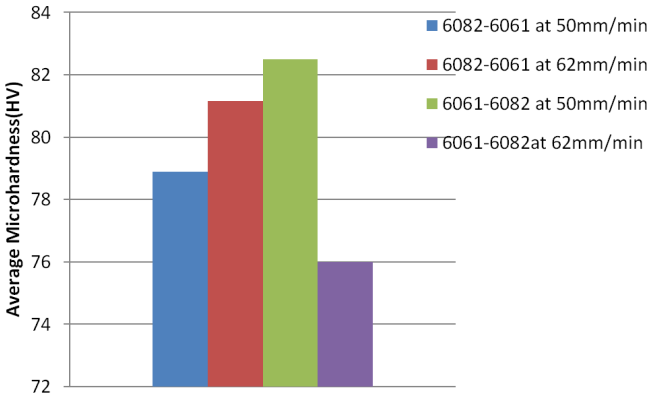

Figure 5: Effect of welding speed on microhardness for dissimilar alloys 6082-6061

3.2 Micro-structural Evolution

Based on optical micro structural characterization of grains and precipitates, three distinct zones have been identified such as weld nugget zone, thermo-mechanically affected zone (TMAZ) and heat affected zone (HAZ). Microstructural details of the base metals (BM) and dissimilar joint are presented in Figs. 6-8. Examination of onion rings in the AA6082- AA6061 at 50mm/min has shown that these onion rings are a result of shell extrusions in the dynamically recrystalized zone (DXZ). In AA6061-6082 at 62mm/min, it can be seen that the root flaw looks like a crack in the root part of the friction stir welds. The root flaw usually occurs if the pin length is too short for the plate thickness being welded, and this may also occur due to low heat input or incorrect tool orientation.

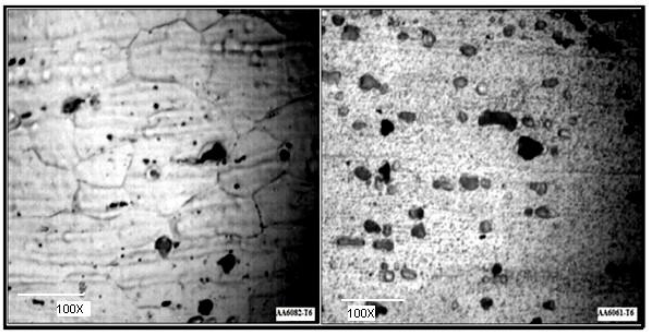

Figure 6: Optical micrograph of base metals AA6082 and AA6061.

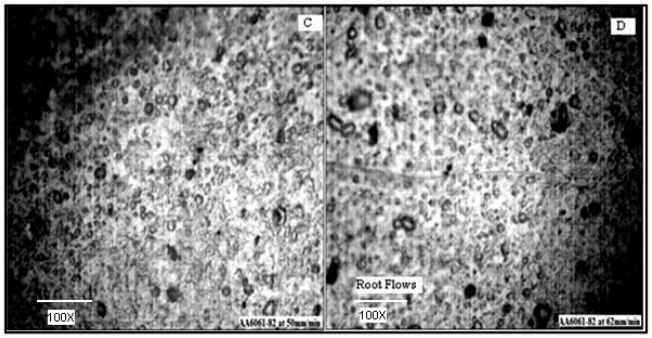

Figure 7: Optical micrograph of AA6082-6061(A) at 50mm/min (B) at 62mm/min

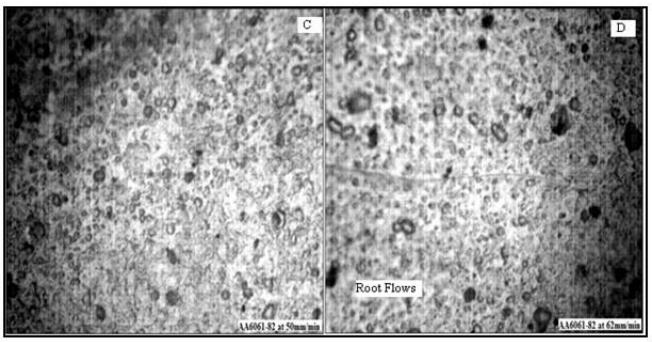

Figure 8: Optical micrograph of AA6061-6082 (C) at 50mm/min (D) at 62mm/min.

3.3 Fractography Analysis

Examination of the tensile fracture surfaces of the FSW joints was done at low magnification as well as at higher magnification in order to identify the fracture mechanisms. According to Figs. 9-10, it may be predicted that the fracture mechanism in the mixing of these alloys will be dimpled rupture. The dimpled rupture fracture mechanism indicates that the fracture occurred with some degree of ductility, but the existence of the defect can always cause a stress concentration around the defect zone during the tension test; therefore, this phenomenon results in a strain locality that is higher than the yield strength in the turbulence zone of the weld, a sudden crack in the specimen, and consequently, a low elongation in the connection.

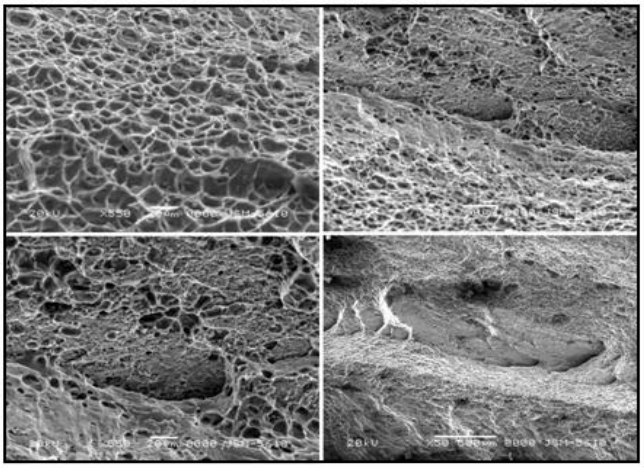

Figure 9: SEM images of tensile fracture surface of 6082-6061 at 50mm/min.

3.4 Corrosion Behaviour

The potentiostatic polarization curves for the base alloy and FSW samples in 3.5%NaCl at room temperature are given in Figs. 11-13. It is shown that the corrosion behavior of base alloy significantly varies from that of welded joints. From Tab. 5 it is observed that the pitting potentials of corrosion tested samples at various process parameters clearly indicated a greater corrosion resistance of weld metal than base metal. This is attributed to the precipitates present in the alloy promote matrix dissolution through selective dissolution of aluminium from the particle. These precipitate deposits are highly cathodic compared to the metallic matrix, which initiates pitting at the surrounding

matrix and also enhances pit growth. During FSW process only coarser precipitates could nucleate and grow but not finer ones. This aids in formation of passive film, which remained more intact on surface of the sample. It is also found that in AA6082-6061 at 50mm/min, the corrosion resistance is very poor. The poor pitting corrosion resistance of weld joint is due to difference in pitting potentials across the weld region or stir nugget because of inhomogeneity of microstructures in those regions. With AA6082 on the advancing side, the corrosion rate is higher with respect to increasing welding speed of the tool while corrosion rate decreased in case of AA6061 on advancing side (Tab. 5). Such dependence of the corrosion behaviour on the material position was observed. All FSW samples show passivation after longer time of exposure to corrosion media. AA6082-61 at 62mm/min has highest active potential (-1.16V). The active Ecorr increased with increasing the weld speed in case advancing and retreating side of 6082T6-6061T6.

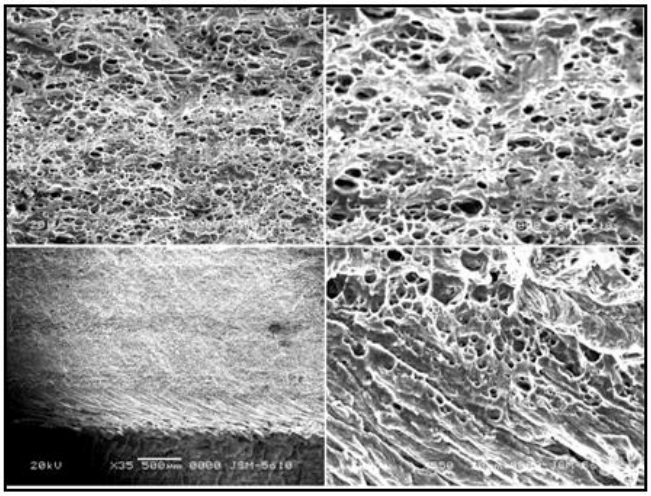

Figure 10: SEM images of tensile fracture surface of 6061-6082 at 62mm/min

Table 5: Result analysis of corrosion test

Material of FSW Joint	Icorr	(μA/cm2)	Ecorr (mV)	Corrosion Rate (mpy)
6082T6-6061T6		55.00	-938	25.14
6082T6-6061T6		3.33	-1160	1.520
6061T6-6082T6		836nA	-732	382 e-3
6061T6-6082T6		1.590	-920	726.661 e-3
AA6082-T6		4.270	-1080	1.95
AA6061-T6		1.820	-1160	832.1 e-3

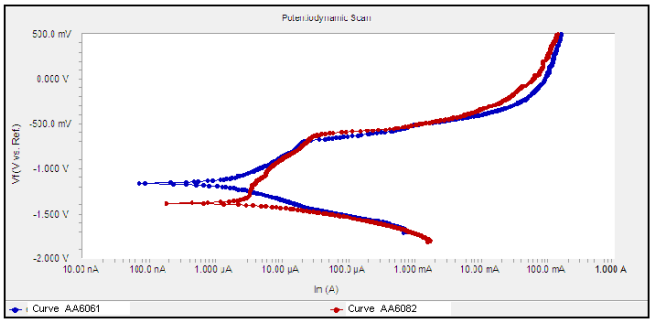

Figure 11: Polarization curves of base metals AA6082 and AA6061

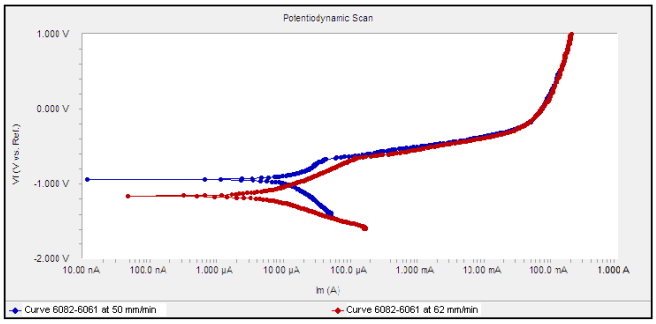

Figure 12: Polarization curves of AA6082-AA6061 at 50-62 mm/min.

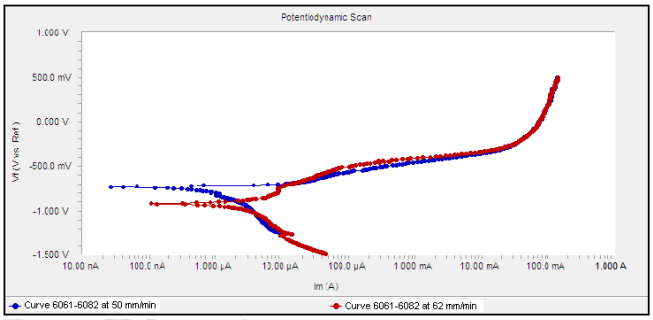

Figure 13: Polarization curves of AA6061-AA6082 at 50-62 mm/min

4. Conclusions

The mechanical and metallurgical behaviour of dissimilar FSW AA6082–AA6061 was studied in this paper. The joints were produced with different alloy positioned on the advancing side of the tool. The joints were realized with a rotation speed of 1600 rpm and by changing the welding speed from 50 to 62mm/min. The downward force was observed to be constant as the welding speed for all the produced joints increases. The tensile strength of the dissimilar joint is lower than that of the parent metal. With the 6082 alloy positioned on the advancing side of the tool, the dissimilar joints exhibited good mechanical properties with respect to AA6061. Microstructural changes induced by the friction stir welding process were clearly identified in this study. Friction stirs welding of dissimilar alloys AA6082T6- 6060T6 resulted in a dynamically recrystalized zone, TMAZ and HAZ. A softened region has clearly occurred in the friction stir welded joints, due to dissolution of strengthening precipitates. With AA6082 on the advancing side; the corrosion rate is higher with respect to increasing welding speed of the tool while corrosion rate decreased in case of AA6061 on advancing side.

References

[1] W. M. Thomas, E. D. Nicholas, Materials & Design, 18 (1997) 269.
[2] W. M. Thomas, E. D. Nicholas, J. C. Needham, M. G. Nurch, P. Temple-Smith, C. Dawes, Patents on Friction Stir Butt Welding, International: PCT/GB92/02203; British: 9125978.8; USA: 5460317, (1991-1995).
[3] W. B. Lee, Y. M. Yeon, S. B. Jung, J. Mater. Sci., 38 (2003) 4183.
[4] W. B. Lee, Y. M. Yeon, S. B. Jung, Scripta Materialia, 49 (2003) 423.

[5] P. Cavaliere, R. Nobile, F.W. Panella, A. Squillace, Int. J. Machine Tools Manufacturing, 46 (2006) 588. [6] P. Cavaliere, A. De Santis, F. Panella, A. Squillace, Material & Design, 30 (2008) 609.
[6] A. Scialpi, M. de Giorgi, L. A. C. de Filippis, R. Nobile, F.W. Panella, Material & Design, 29 (2008) 928. [8] L. E. Murr, N. A. Rodriguez, E. Almanza, C. J. Alvarez, J. of Material Science, 40 (2005) 4307
[7] J. H. Ouyang, R. Kovacevic, J. Material Engineering, 11 (2002) 51.
[8] T. L. Dickerson, J. Przydatek, Int. J. Fatigue, 25 (2003) 1399.
[9] C.S. Paglia, K.V. Jata, R.G. Buchheit, Material Science Engineering A, 424 (2006) 196.
[10] R.W. Fonda, P.S. Pao, H.N. Jones, C.R. Feng, B.J. Connolly, A.J. Davenport, Material Science Engineering A, 519 (2009) 1.
[11] D.A. Wadeson, X. Zhou, G.E. Thompson, P. Skeldon, L. Djapic Oosterkamp, G. Scamans, Corrosion Science, 48 (2006) 887.
[12] M. Jariyaboon, A.J. Davenport, R. Ambat, B.J. Connolly, S.W. Williams, D.A. Price, Corrosion Science, 49 (2007) 877.
[13] P. S. Pao, S. J. Gill, C. R. Feng, K. K. Sankaran, Scripta Materiala, 45 (2001) 605.
[14] K. Surekha, B. S. Murty, K. Prasad Rao, Solid State Sciences, 11 (2009) 907